THE CALCULATION AND THE MEASUREMENTS OF THE ELETTRA MAGNETS

G. Petrucci, S. De Panfilis*, F. Gnidica*, G. Stefanini
CERN, CH 1211 Geneve 23 - Switzerland
* Sincrotrone Trieste - Padriciano 99 - 34012 TS - Italy

The Magnetic Field Measuring System

Two measuring systems for the ELETTRA ring magnets have been developed, to comply with the requirements of 0.01% measurement accuracy for the dipole gradient and, respectively, for the relative amplitudes of harmonic components in quadrupoles and sextupoles. Each setup consists of: i) a magnet support with precision adjustments for accurate alignment, ii) a field measuring bench and iii) an on-line data acquisition system.

The adjustable supports

The supports allow for accurate linear and angular translations of the magnets in the horizontal and in the vertical plane, as required by the alignment procedure outlined in the following sections.

The field measuring benches

The quadrupole and sextupole: The amplitudes of the harmonic field components are measured by the well-known technique of the rotating coil. In our case, the coil consists of a multi-layer printed circuit board, with a total of 8 turns for a length of 700 mm. The dimensional tolerances of the circuit are ≈ 0.01 mm; a clearance of 0.5 mm is left between the outer conductor position and the pole surface. The circuit is split lengthwise in two identical sections; the two signals are subtracted for alignment purposes, and added for normal measurements. To obtain stiffness and dimensional stability, the printed circuit is glued and encased in a fiberglass tubular structure (figure 1).

The measuring bench also includes alignment tools (laser and PSD) to set the survey reference marks on each unit, once the symmetry planes have been determined by the field measurement (figure 2).

The dipole: The dipole bench (figure 3) makes use of a Hall plate measuring module consisting of an array of 15 plates, temperature stabilized, mounted along a line in the horizontal plane, at a pitch of 10 mm (constant to within the uncertainty in the actual sensitive spot position on each plate). The module (figure 4) can be accurately positioned in the magnet gap by a three axis gear with programmable stepping motor controls, with an accuracy of ≈ 0.01 mm.

This measuring bench is also equipped with suitable alignment tools.

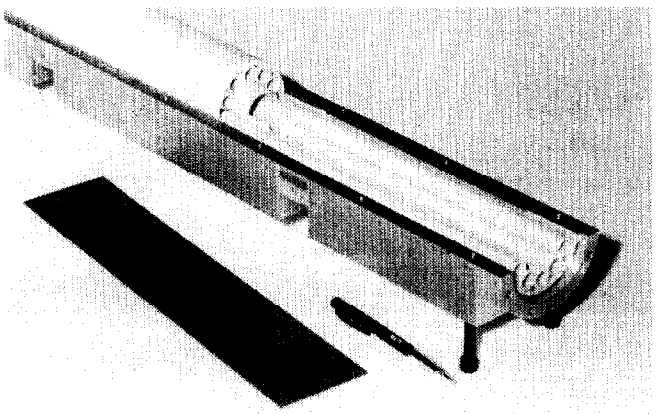

Figure 1: Exploded view of the fiberglass tube and one section of the printed circuit before being assembled.

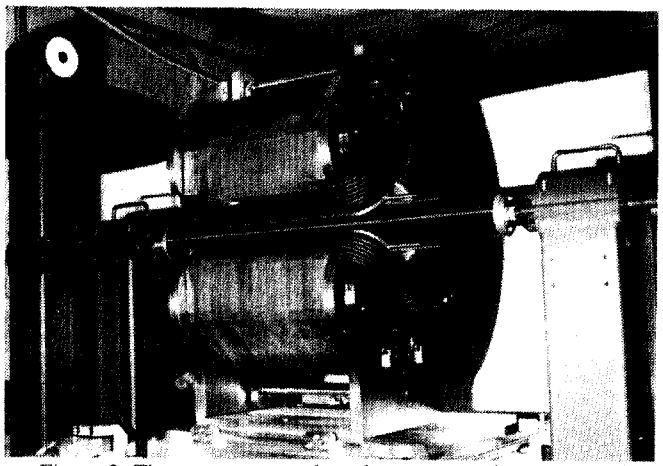

Figure 2: The prototype quadrupole magnet on its support. The integrating coil is shown in its measuring position inside the magnet. The PSD support is also shown on the high left corner.

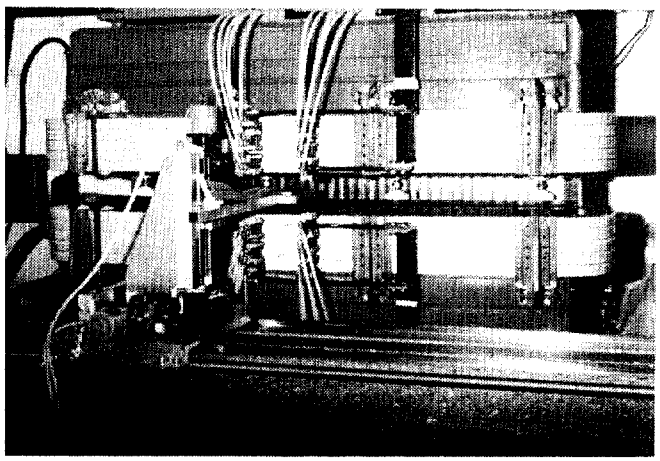

Figure 3: The prototype dipole on its support and the measuring bench with the three axis gear and the measuring probe.

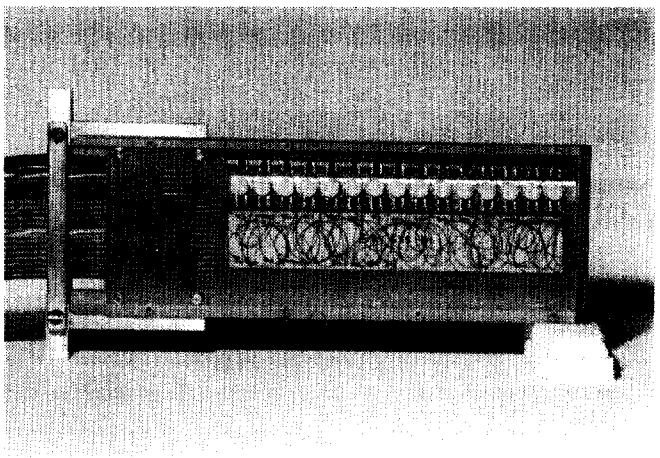

Figure 4: The Hall plate measuring module.

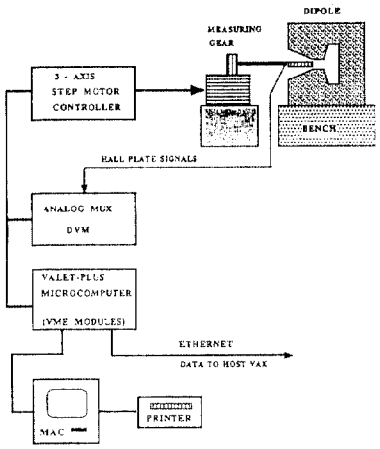

Figure 5a: The block diagram for the quadrupole and sextupole measuring system.

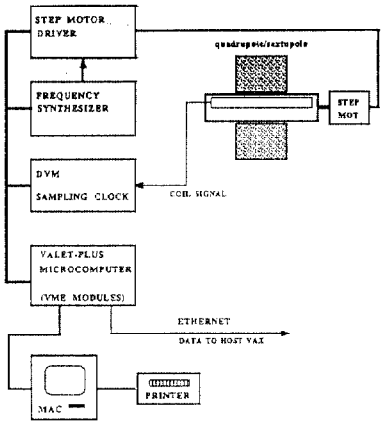

Figure 5b: The block diagram for the dipole measuring system.

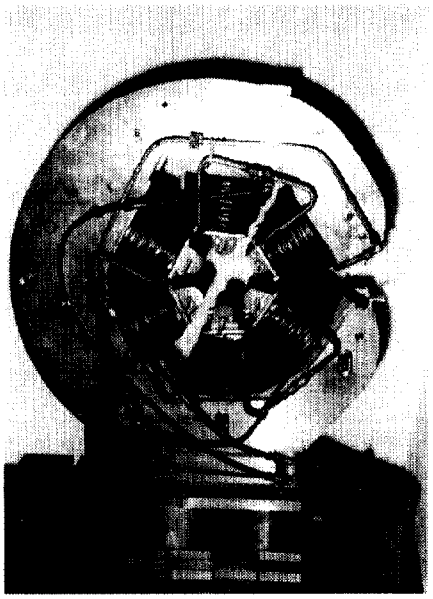

Figure 6: The prototype sextupole.

The on-line data acquisition

The positioning of the probes, the triggering of the data acquisition and the data acquisition itself are controlled by a VME-based ValetPlus microcomputer (CERN-DD development), together with a programmable data acquisition control unit (HP 3852A). A Macintosh is used as intelligent terminal.

A block diagram of the data acquisition system for the quadrupoles/sextupoles is shown in figure 5a. An interesting feature of this system is the method used for driving the rotating coil. A stepping motor, with a 100:1 precision reduction gear, drives the coil at constant angular speed. The data acquisition is triggered at a well defined angular position of the coil; the DVM then measures and stores in a buffer a number of samples (typically 512) spaced by a time interval (pacer clock) such that the total time for the measurement equals the time for one complete rotation of the coil inside the magnet (≈ 50 sec). The data are then read-out and Fourier analyzed (FFT algorithm). The peak signal amplitude of the main component is ≈ 3 mV. The relative amplitudes of the harmonic components are measured to an accuracy of $\approx 10^{-4}$.

A block diagram of the data acquisition system for the dipole is shown in figure 5b. Low-noise analog multiplexers are used to measure the Hall plate signals with a resolution of 1 μV. The field gradients at each plate position are measured by performing a precise (to 0.01 mm) horizontal translation of the carriage, orthogonal to the dipole longitudinal axis. By fitting and integrating the measured values, a complete field map is then derived.

Magnetic Field Calculation

The magnets simulation programs Poisson (2D) and Tosca (3D) (Vector Field Ltd.) have been used to calculate the optimal design for the magnets. The usage of the 3D program was important due to the shortness of our quadrupoles and sextupoles.

Results for the CERN Model Quadrupole and Sextupole

Measurements and calculations have been performed on the CERN prototype quadrupole (figure 2) and sextupole (figure 6) that have being built on an early design to test the quality of the calculation and of the measuring systems. Results on the calculated integrated value of the field along the longitudinal axis of the magnet are shown in figures 7 and 8 respectively. In Tables 1 and 2 the comparison between the calculated and the measured values is presented.

In the quadrupole the agreement is quite good for the allowed 6th and 20th harmonics . The 4th and 8th harmonics come from assembling asymmetry for the measured values, and geometrical asymmetry for the calculated values due to the unusual design. For the sextupole similar comments can be made.

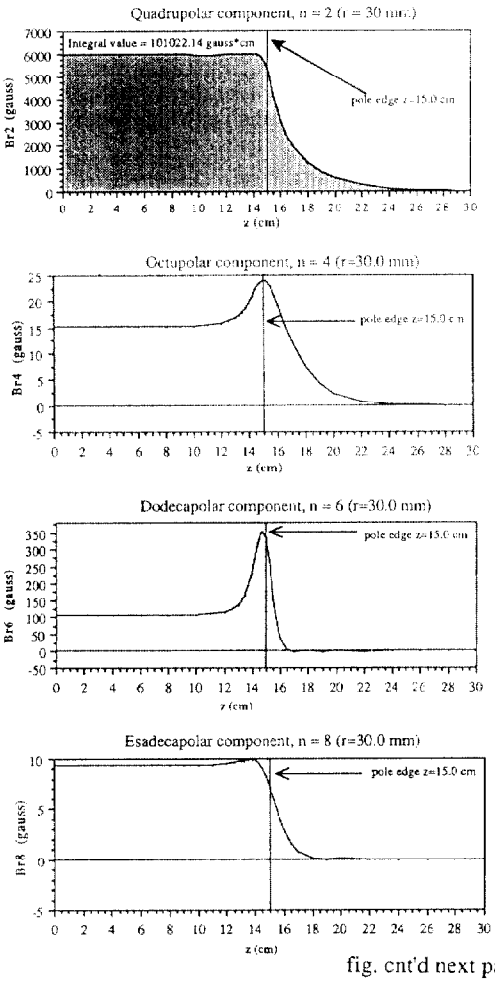

fig. cnt'd next page

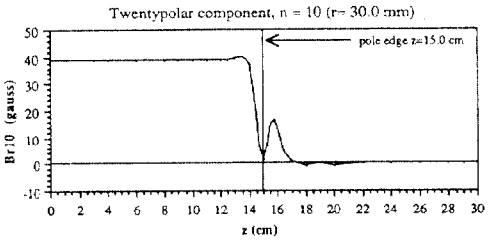

Figure 7: Calculated harmonic components along the longitudinal axis in the quadrupole.

TABLE 1

Order of component n	Computed ratio $\lvert J_n / J_2 \rvert$	Measured ratio $\lvert J_n / J_2 \rvert$
4	$3.0\ 10^{-3}$	$5.7\ 10^{-3}$
6	$2.03\ 10^{-2}$	$2.07\ 10^{-2}$
8	$1.5\ 10^{-3}$	$1.9\ 10^{-3}$
10	$5.7\ 10^{-3}$	$5.2\ 10^{-3}$

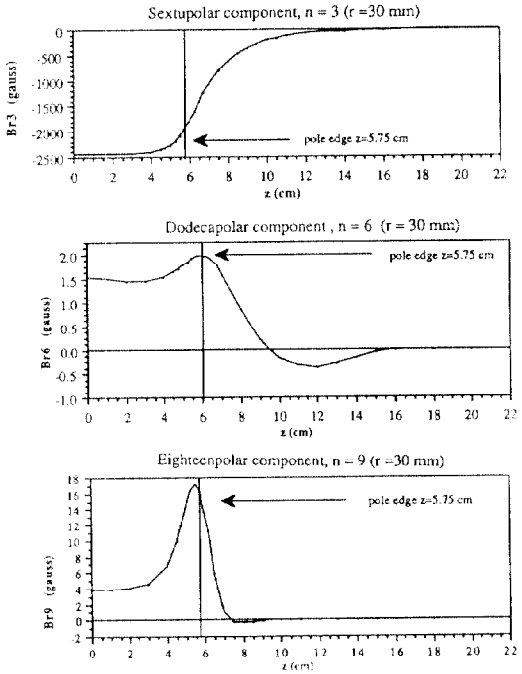

Figure 8: Calculated harmonic components along the longitudinal axis in the sextupole.

TABLE 2

Order of component n	Computed ratio $\lvert J_n / J_3 \rvert$	Measured ratio $\lvert J_n / J_3 \rvert$
6	$0.6\ 10^{-3}$	$1.2\ 10^{-3}$
9	$2.8\ 10^{-3}$	$2.7\ 10^{-3}$
12	$0.0\ 10^{-3}$	$0.1\ 10^{-3}$
15	$0.0\ 10^{-3}$	$0.0\ 10^{-3}$

Optimization for the quadrupole profile

In figure 9 the optimized profile for the quadrupole is shown. The results deriving from this profile are shown in figure 10, and in table 3 the relative amplitudes of the harmonic components are given.

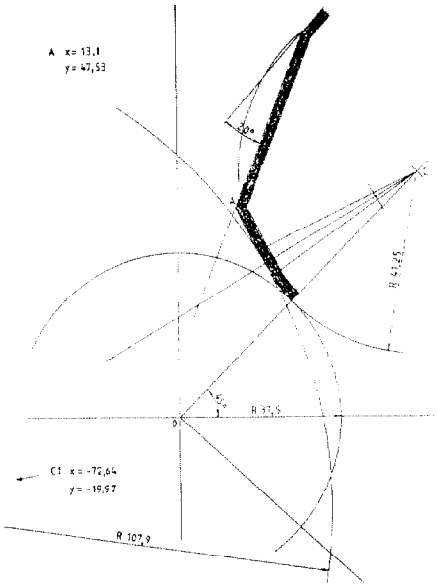

Figure 9: The construction drawing for the optimized profile.

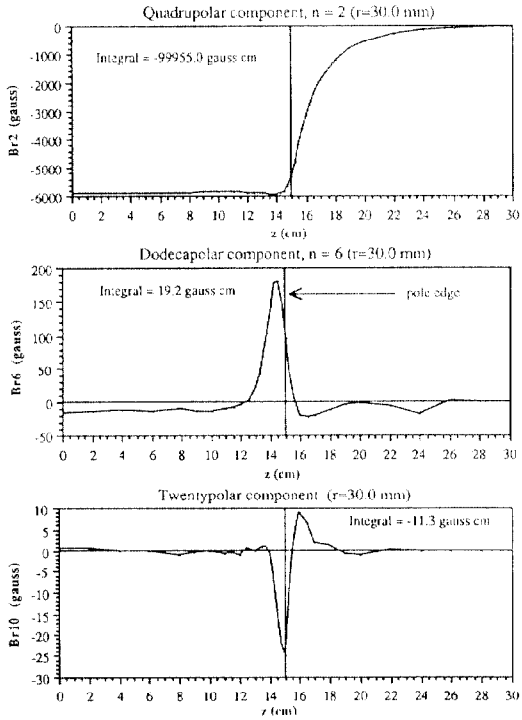

Figure 10: Calculated harmonic components along the longitudinal axis in the optimized quadrupole. In this calculation the pole tips were included.

TABLE 3

Order of component n	Computed ratio $\lvert J_n / J_2 \rvert$	Max. allowed value $\lvert J_n / J_2 \rvert$
6	$1.9\ 10^{-4}$	$9.0\ 10^{-4}$
10	$1.1\ 10^{-4}$	$3.0\ 10^{-4}$

Acknowledgement

The authors are thankful to the EP Technical Drawing Office and the Workshop teams, and to the technical staff of the EP-GE group of CERN, for their contribution to the drawing, design and assembly of the magnet models and the measuring systems.